[3] N. D. Veksler: Sound wave scattering by circular cylindrical shells. Wave Motion 8 (1986) 525–536.

[4] H. Überall, L. R. Dragonette, L. Flax: Relation between creeping waves and normal modes of vibration of a curved body. J. Acoust. Soc. Am. 61 (1977) 711–715.

[5] V. Twersky: Scattering of waves by two objects. – In: Electromagnetic wave. Conference Proceedings. R. E. Langer (ed.) 1961. 361–389.

[6] G. Dumery: Sur la diffraction des ondes sonores par des grilles ou des réseaux d'obstacles. Acustica 18 (1967) 334–341.

[7] C. Audoly, G. Dumery: Modeling of compliant tube underwater reflectors. J. Acoust. Soc. Am. 87 (1990) 1841–1846.

[8] J. W. Young, J. C. Bertrand: Multiple scattering by two cylinders. J. Acoust. Soc. Am. 58 (1975) 1190–1195.

[9] J. P. Sessarego, J. Sageloli: Diffusion acoustique par deux coques cylindriques parallèles: comparaison expérience-théorie. J. Acoustique 5 (1992) 463–477.

[10] M. Abramowitz, I. Stegun: Handbook of mathematical functions. Dover Publications. Inc. New York. 1972.

[11] B. Peterson, S. Ström: Matrix formulation of acoustic scattering from an arbitrary number of scatterers. J. Acoust. Soc. Am. 56 (1974) 771–780.

[12] S. K. Numrich, N. K. Dale, L. R. Dragonette: Advances in fluid-structure interaction. – In: PVD. Vol. 78 / AMD Vol 64.59. G. C. Everstine, M. K. Au-Yang (eds.). Am. Soc. Mech. Eng. New York. 1984.

[13] P. Delestre, J. L. Izbicki, G. Maze, J. Ripoche: Excitation acoustique impulsionnelle d'une plaque élastique immergée: application à l'isolement des résonances. Acustica 61 (1986) 83–85.

[14] M. de Billy: Determination of the resonance spectrum of elastic bodies via the use of short pulse and Fourier transform theory. J. Acoust. Soc. Am. 79 (1986) 219–221.

[15] M. Talmant, J. L. Izbicki, G. Maze, G. Quentin, J. Ripoche: External wave resonances on thin cylindrical shells. J. Acoustique 4 (1991) 509–523.

[16] P. L. Marston, N. H. Sun: Resonance and interference scattering near the coincidence frequency of a thin spherical shell: an approximate ray synthesis. J. Acoust. Soc. Am. 92 (1992) 3315–3319.

[17] E. Kheddioui, P. Pareige, J. M. Conoir, J. L. Izbicki, J. Ripoche: Experimental manifestation of the resonant interaction between two close elastic shells. 19th Ultrasonics International Conference, Vienna. Conference Proceeding. Butterworth 1993 475–478.

[18] E. Kheddioui, P. Pareige, J. L. Izbicki: Experimental resonant scattering by two cylindrical shells in an exlipsed configuration. Acoustics Letters 7 (1993) 157–162.

[19] P. L. Marston: G. T. D. for backscattering from elastic spheres and cylinders in water and the coupling of surface elastic waves with the acoustic field. J. Acoust. Soc. Am. 83(1) (1988) 25–37.

# On the Relation Between Surface Waves on a Bubble and the Subharmonic Combination-Frequency Emission

D. G. Ramble, A. D. Phelps, T. G. Leighton

The Institute of Sound and Vibration Research. The University of Southampton, Southampton SO17 1BJ, UK

## Abstract

The characterisation of bubbles using a two-frequency excitation technique is known to accurately detect and size certain bubble samples. This is done through the generation of a signal at $\omega_i \pm \omega_p/2$ when the bubble is insonified by a fixed MHz imaging signal $\omega_i$ and a variable pumping frequency $\omega_p$ tuned to the bubble's resonance. Recent work has suggested that the principal mechanism for the generation of the $\omega_i \pm \omega_p/2$ signal is linked to the onset of surface waves on the bubble's surface. This paper strengthens this argument through the comparison of published experimentally measured thresholds for the $\omega_i \pm \omega_p/2$ signal with recent theoretical models which predict the driving sound field pressure amplitudes required for the onset of surface waves on a spherical surface.

## 1. Introduction

The ability to detect and make measurements of gas/vapour bubble populations in fluid media has applications in a wide range of fields (see, for example, [1]). Acoustic methods are particularly potent, as the high impedance mismatch at the bubble surface scatters incident acoustic energy very effectively. Additionally, when driven acoustically, bubbles can pulsate like single degree of freedom oscillators, with the gas inside the bubble providing the stiffness element and the water surrounding the bubble acting as the mass element. These

pulsations exhibit strong resonance characteristics [2]. and from the value of a bubble's resonance frequency its size can be readily obtained.

One particular acoustical method uses a two-frequency excitation comprising a fixed imaging frequency $\omega_i$ of MHz order and a variable pump frequency $\omega_p$ tuned to the kHz resonance frequency of the bubble. The high frequency signal scatters geometrically from the bubble, with the strength of the scattered signal related to the target area which the bubble presents to the incident beam. If, however, the bubble is simultaneously being driven to pulsate close to its resonance frequency by the pump signal, the target area presented to the imaging signal will vary in time; thus the scattered signal will be amplitude modulated at the pump frequency. This signal coupling will result in the generation of sum and difference signals at $\omega_i \pm \omega_p$. However, other signals at $\omega_i \pm \omega_p/2$ etc. have also been observed in the backscattered spectrum if the amplitude of the pump signal exceeds a certain value [3].

It became clear that the appearance of the signal at $\omega_i \pm \omega_p/2$ is a particularly accurate indicator of the resonance frequency of the bubble. and thus its size [3]. The mechanism for the generation of this signal has been the subject of recent work [3, 4, 5]. This short communication reinforces these workers' suggested explanation that surface waves on the bubble are responsible, through the comparison of previously published experimental work with a new theoretical approach to modelling the onset of these surface waves. The text finishes by demonstrating the lightly damped nature of these waves through recent experimental measurements.

## 2. Proposed mechanisms for the production of the combination-frequency subharmonic emission

Recent studies [3, 4] have argued that the $\omega_i \pm \omega_p/2$ signal must result from some subharmonic component in the bubble oscillation. These studies have shown that the subharmonic combination frequency signal is parametric in nature, in that the bubble must be driven by a suitably high pressure field before the signal is generated. The workers experimentally measured the amplitude of the driving pump sound field at this onset threshold for 28 different tethered bubbles resonant between 2 kHz and 3.2 kHz. This threshold was at approximately 35 Pa over the range of bubble sizes considered. From this it was argued that if the mechanism responsible for the

direct subharmonic emission has the same onset threshold, then it is probable that this mechanism it also linked to the subharmonic combination frequency signal

Neppiras [6] suggested three possible mechanisms for the direct subharmonic emission. The first was based around the work of Eller and Flynn [7], who theorised that the emission was due to the non-linear oscillations of the bubble's volumetric pulsations, though the minimum threshold for the onset of this effect occurred at a frequency of twice the resonance frequency of the bubble. The second was also linked to the nonlinear volumetric pulsations of the bubble; Lauterborn [8] suggested that as the bubble was driven harder there was a potential for the system to become more chaotic. The progression of the bubble's response into a state of chaos was carried out by a series of bifurcations, the first of which resulted in a period doubling. However subsequent analysis [4] has shown that the calculated pressure threshold required to cause a subharmonic emission by these effects on bubbles resonant at several kHz was ~ $10^5$ Pa, and so is several orders of magnitude greater than the experimentally observed combination-frequency subharmonic signal [3].

The third mechanism suggested by Neppiras concerned the onset of surface waves. These were first noted by Faraday [9] who observed a plane water surface set in motion over vibrating plates and reported the appearance of waves at half the driving frequency. Such surface oscillations have also long been associated with stable cavities, since being first recorded by Kornfeld and Suvarov [10]. Hullin [11] used stroboscopic illumination to show that these surface deformations occurred at exactly half the excitation frequency, and so the wave which was stimulated was indeed subharmonic in time. Phelps and Leighton [3, 4] calculated the onset pressure for the driving pump sound field required to stimulate these Faraday waves on a plane surface, and this showed a good correlation with the onset pressure amplitude measured experimentally for the 28 bubbles between 2 and 3.2 kHz.

## 3. Surface wave theory for spherical cavities

As a refinement to the plane surface approximations in the work of Phelps and Leighton [3, 4], the work has been extended to theoretically investigate the generation of surface waves of order one-half on a spherical cavity. The theoretical pulsation amplitude, $A_t$, required to generate such surface waves has been derived by Francescutto and Nabergoj [12] as:

$$A_t = \sqrt{\frac{2\left[(\omega_n^2 - \omega^2/4)^2 + \beta_n^2(\omega_n^2 - \beta_n^2)\right]}{\left[-3\omega_n^2 + 4\beta_n^2 + (n+1/2)\omega^2\right]^2 + x_n^2\omega^2}}, \quad (1)$$

where $n$ is the integer number of the particular mode being stimulated, and:

$$\omega_n^2 = \frac{(n-1)(n+1)(n+2)\sigma}{\rho R_0^3}, \quad (2)$$

$$\beta_n = \frac{(n+2)(2n+1)\mu}{\rho R_0^2}, \quad (3)$$

$$x_n = \frac{3(n+2)\mu}{\rho R_0^2} \quad (4)$$

In these expressions, $\sigma$ is the value for the surface tension, $\rho$ is the liquid density, $R_0$ is the equilibrium bubble radius and $\mu$ is the shear viscosity coefficient.

To convert this pulsation amplitude threshold into a driving sound field pressure amplitude it is necessary to relate the radial displacement of the bubble, $R_{\epsilon 0}$, to the incident pressure amplitude, $P_A$. This relationship is straightforward to derive (see for example [1]) and is given as:

$$R_{\epsilon 0} = \frac{P_A}{R_0\rho} \frac{1}{\sqrt{(\omega_0^2 - \omega^2)^2 + (\omega^2 d_{tot})^2}}, \quad (5)$$
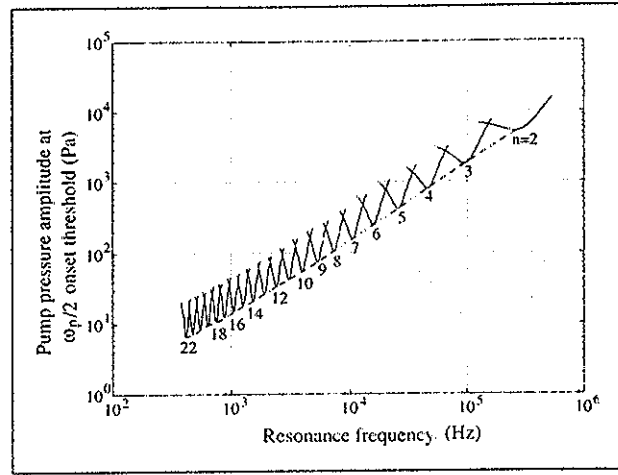


Figure 1. Calculated driving pressure amplitude, in Pa, versus resonance frequency, to excite surface waves on air bubbles in water insonified at their resonance frequency. Number of each curve refers to the particular surface mode. Dashed line corresponds to "effective" threshold

where $d_{tot}$ is the total non-dimensional damping coefficient signifying viscous, radiation, and thermal losses. This expression is valid when $R_{\epsilon 0} \ll R_0$ and when the radius of the bubble is much smaller than the wavelength of the incident sound field. It also assumes that the bubble is undergoing volumetric pulsations. This last assumption is valid when considering the *threshold* for the onset of surface waves when the pump signal amplitude is increased from sub-threshold conditions (as was the experimental protocol of Phelps and Leighton [3]). The damping term in equation (5) can be evaluated using the expressions for thermal, viscous, and radiation damping derived by Eller [13]. By incorporating the thermal conduction losses in the polytropic index the total damping can be expressed as:

$$d_{tot} = \frac{4\omega\mu}{3\kappa p_0} + \frac{\rho}{3\kappa p_0}\frac{(R_0\omega)^3}{c}, \quad (6)$$

where $p_0$ is the hydrostatic pressure at the bubble, $c$ is the speed of sound in the liquid and $\kappa$ is the polytropic index of the pulsations. Thus, by replacing $R_{\epsilon 0}$ by the expression for the threshold displacement in equation (5), the driving sound field pressure threshold, $P_T$, for surface wave generation of order one-half is found to be:

$$P_T = P_A = \frac{3\kappa p_0 d_{tot} A_t}{R_0}. \quad (7)$$

From this equation a plot (Figure 1) can be made for the threshold driving pressure as a function of resonant frequency for the surface modes (with $n$ up to 22) for air bubbles in water. From Figure 1 it can be seen that the most readily excited modes are those whose frequencies coincide with a subharmonic of the generation frequency. For instance, a bubble resonant just above 10 kHz would most easily excite the $n = 7$ surface mode when the driving pressure exceeded around 180 Pa. However, in the region between these minima Francescutto and Nabergoj [12] note that other minima will presumably appear corresponding to zones of instability. These were not taken into account in their first order analysis and so an "effective" threshold is also plotted on Figure 1 as a dashed line.

A comparison of the calculated threshold from the spherical-surface wave theory with the experimentally measured $\omega_i \pm \omega_p/2$ signal threshold is shown in Figure 2 (dashed line). In addition, the theoretical threshold calculated from the plane-surface theory presented by Phelps and Leighton [3, 4] is also given (unbroken line). It is evident that the revised theory shows excellent agreement between the onset of the surface waves and the threshold for the subharmonic combination frequency emission, which strengthens the argument that the onset of surface waves is the principal mechanism responsible for the subharmonic combination-frequency signal
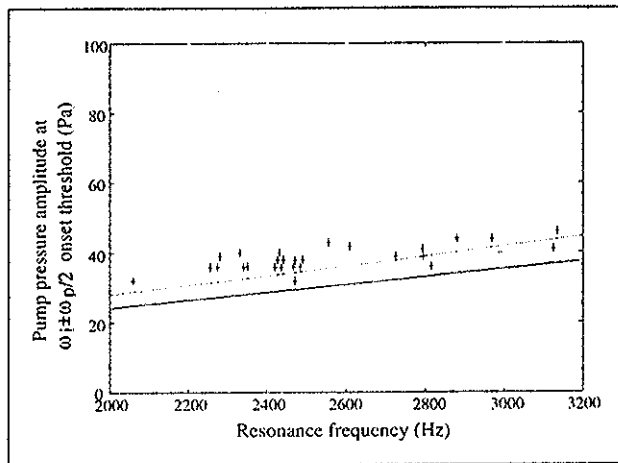
Figure 2 Plot showing the driving pressure thresholds for order one-half subharmonic excitation of air bubbles resonant in the frequency range 2000 to 3200 Hz at a depth of 15 cm in water. The solid line is the subharmonic threshold calculated from plane-surface theory, the dashed line is the threshold calculated from spherical-surface theory and the crosses (+) are published [3] experimentally measured thresholds for the $\omega_i \pm \omega_p/2$ signal.
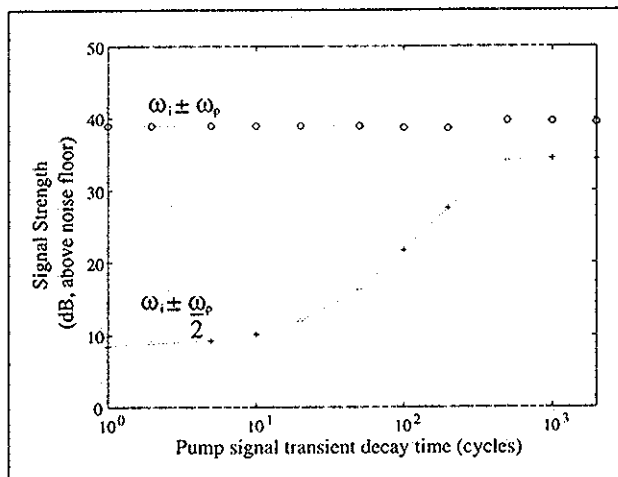


Figure 3 Plot showing the effect of different transient decay delay times between the start of bubble insonification and data acquisition. The data shows the maximum amplitudes of the subharmonic and the fundamental combination frequency signal when the 2700 Hz resonant bubble is driven at 50 Pa. The decay time is measured in cycles of the pumping signal, and the ordinate shows the amplitude of the monitored signal above the noise floor.

## 4. Discussions and Conclusions

This short communication has presented a new theoretical treatment for the threshold pump signal acoustic pressure amplitude required to stimulate surface waves on a spherical bubble. This theory has been shown to be in excellent agreement with the previously measured threshold for the generation of a combination frequency subharmonic signal.

The results from previous work have shown the $\omega_i \pm \omega_p/2$ signal not only to be an unambiguous indicator of a resonant bubble [3], but also potentially allowing a far more accurate estimate of a bubble's resonance frequency than any other signals related to the volumetric change of the bubble (affording better than 1% accuracy in the estimates of the resonance frequency [3]). This is because of the different damping mechanisms involved in volumetric pulsations and the surface waves: the damping of the latter is very much lighter

and thus a $\omega_i \pm \omega_p/2$ signal can only be stimulated from a bubble when driven very close to its resonance frequency. Thus when monitoring the subharmonic combination frequency signal ideally a period of insonification is required before the data is acquired in order to allow for transients to decay. This is demonstrated in Figure 3, which shows how a tethered 2700 Hz resonant bubble reaches its maximum subharmonic combination-frequency amplitude only after 400 cycles of the driving pumping frequency. This has obvious implications to moving bubble detection where no such delay can be afforded.

Additionally, however, the ability of the $\omega_i \pm \omega_p/2$ signal to propagate to distance needs to be considered, as the subharmonic signal itself does not, to behave as a monopole source requires a volumetric change in the bubble pulsation which the surface distortions do not demonstrate. Earlier, it was discussed that the source of the sum and difference terms in the scattered spectrum when undergoing two frequency excitation derives from the amplitude modulation of the scattered high frequency signal by a varying target area, the pulsating bubble. Thus the bubble's ability to couple effectively with the imaging signal is actually a function of the geometrical cross-sectional area of the target presented to the high frequency imaging beam and is not due to the volumetric changes of the bubble. Therefore, the subharmonic variation of the cross-sectional area of the bubble, caused by the propagation of surface waves around the bubble wall in turn causes the amplitude of the high frequency ultrasound beam to be amplitude modulated with a $\omega_p/2$ component. This signal can then detected by the receiving high frequency transducer.

## References

[1] T. G. Leighton: The acoustic bubble. Academic Press, London, UK, 1994.
[2] M. Minnaert: On musical air-bubbles and the sounds of running water. Phil. Mag. 16 (1933) 235–248.
[3] A. D. Phelps, T. G. Leighton: High resolution bubble sizing through detection of the subharmonic response with a two frequency technique. J. Acoust. Soc. Am. 99 (1996) 1985–1992.
[4] A. D. Phelps, T. G. Leighton: The subharmonic oscillations and combination frequency emissions from a resonant bubble. Acta Acustica 83 (1997) 59–66.
[5] A. O. Maksimov: On the subharmonic emission of gas bubbles under two frequency excitation. Ultrasonics 35 (1997) 79–86.
[6] E. A. Neppiras: Acoustic cavitation. Physics Reports 3 (1980) 159–251.
[7] A. I. Eller, H. G. Flynn: Generation of subharmonics of order one-half by bubbles in a sound field. J. Acoust. Soc. Am. 46 (1969) 722–727.
[8] W. Lauterborn: Numerical investigation of nonlinear oscillations of gas bubbles in liquids. J. Acoust. Soc. Am. 59 (1976) 283–293.
[9] M. Faraday: On the forms and states assumed by fluids in contact with vibrating elastic surfaces. Philos. Trans. Roy. Soc. 121 (1831) 319–340.
[10] M. Kornfeld, L. Suvarov: On the destructive action of cavitation. J. Applied Physics 15 (1944) 495–506.
[11] C. Hullin: The stability of pulsating air-bubbles in water. Acustica 37 (1977) 64–73.
[12] A. Francescutto, R. Nabergoj: Pulsation amplitude threshold for surface waves on oscillating bubbles. Acustica 41 (1978) 215–220.
[13] A. I. Eller: Damping constants of pulsating bubbles. J. Acoust. Soc. Am. 47 (1970) 1469–1470.